JOURNAL OF THEORETICAL BIOLOGY

Geometric Optical Optimization of the Corneal Lens of Notonecta glauca

GÁBOR HORVÁTH

Hungarian Academy of Sciencies, Central Research Institute for Physics, Biophysical Group, H-1525 Budapest, P.O.B. 49, Hungary

(*Received* 22 *June* 1988, *and accepted in revised form* 15 *March* 1989)

Academic Press
Harcourt Brace Jovanovich, Publishers
London San Diego New York
Boston Sydney Tokyo Toronto

J. theor. Biol. (1989) **139,** 389–404

Geometric Optical Optimization of the Corneal Lens of *Notonecta glauca*

GÁBOR HORVÁTH

Hungarian Academy of Sciencies, Central Research Institute for Physics, Biophysical Group, H-1525 Budapest, P.O.B. 49, Hungary

(*Received* 22 *June* 1988, *and accepted in revised form* 15 *March* 1989)

The optimal shape of the corneal lens of the water bug backswimmer (*Notonecta glauca*) and the optimal shape and position of the thin transition layer between the distal and proximal units of its cornea are theoretically determined. Using a geometric optical method, first the shape of a geometric interface between the lens units is determined, which eliminates the longitudinal spherical aberration. This interface is investigated for differently formed thick lenses when the medium in contact with the entrance surface of the lens is water or air. The optimal transition layer for the amphibious backswimmer is that, the boundaries of which are the theoretical interfaces for water and air, and the refractive index varies continuously in it.

The optimal shape of the corneal lens is determined, with the disadvantageous lenses, with respect to the possible minimal spherical aberration and amount of reflected light from the transition layer, being rejected. The optimal position of the transition layer in the cornea can be obtained from the minimization of the amount of diffracted light on the marginal connection of the layers.

The optimal corneal lens for backswimmer has ellipsoid boundary surfaces; the optimal transition layer in it is thin bell-shaped, at the marginal connection of which there is no dimple, the maximum of the layer is on the margin of the cornea. The shape of the theoretically optimal corneal lens, the shape and position of the theoretically optimal transition layer agree well with those of *Notonecta glauca.*

The question posed, the geometric optical method used and the results presented are of general importance, and not only with respect to vision in the bug *Notonecta,* but also in the fossil trilobites, or in the wave guide theories which have been employed in similar modelling problems, in design of system of lenses without spherical aberration, for example.

1. Introduction

The structure of the dioptric apparatus of the amphibious water bug backswimmer (*Notonecta glauca*) is well-known, and is investigated profoundly by Schwind (Schwind, 1980, 1983, 1985; Schwind *et al.*, 1984). He showed experimentally that the thin transition layer between the two units of the backswimmer's corneal lens eliminates the longitudinal spherical aberration.

Schwind made a simple numerical calculation to determine the approximate shape of this transition layer (Schwind, 1980), which was considered as an exact geometrical interface. His computer program used to calculate the ray paths was based on a repeated application of refraction law for passage of rays through centered refractive spherical surfaces. The obtained interfacial curve (section of the transition interface) consisted of 1100 segments of circles. The position of their centres along the optical

0022-5193/89/150389+16 $03.00/0

axis and their radius of curvature were determined iteratively so that the deviation of their focal points from that of a preset value was always smaller than $10^{-4} f$, where f is the focal length. This iterative method is difficult and slow; it does not allow for quickly determining the theoretical shape of the transition layer for differently shaped corneal lens.

In this work a more general and quicker method is given to solve the geometric optical problem of the shape of the transition interface of thick lenses without longitudinal spherical aberration. The optimal thickness and shape of the transition layer, its optimal position in the cornea and the optimal shape of the corneal lens of *Notonecta glauca* are determined on the basis of this method.

The question posed, the geometric optical method used and the results presented are of general importance, and not only with respect to vision in the bug *N. glauca*, but also in the fossil trilobites (Clarkson, 1973; Levi-Setti, 1975) or in the wave guide theories employed in similar geometric optical modelling problems, in design of system of lenses without spherical aberration (for example, Born & Wolf, 1964; Luneburg, 1964; Stravroudis, 1972; Chang & Stravroudis, 1980).

2. The Eye of *Notonecta glauca*

The dioptric apparatus of the eye of *N. glauca* consists of the cornea and the crystalline cells, at the proximal end of which an open rhabdom begins. The acone type eye has four crystalline cells in place of a secreted cone, which are optically homogeneous (Schwind, 1980).

The cornea consists of two homogeneous units. In the distal unit the refractive index is high and in the proximal one it is low. The two units are separated by a narrow transition layer, the refractive index of which varies continuously and its thickness increases from the optical axis towards the margin of the cornea (Fig. 1, Schwind, 1980, 1985).

The entrance surface of an individual corneal lens is only slightly convex: therefore there is little change in the position of the plane of focus in the eye when the amphibious bug leaves the water. In Fig. 1 refractive indices and shapes of refracting surfaces of the dioptric apparatus are indicated. Measurements of the intact corneal lenses confirmed that they have only very little longitudinal spherical aberration (Schwind, 1985).

In a horizontal section through the eye one finds ommatidia of radially-symmetric structure (Fig. 1) only in the middle region, between the median and lateral peripheral zones. In these peripheral regions the dioptric apparatus is slanted. The diameter of the corneal lenses is quite small, 40 μm (Schwind, 1980).

All the peripheral rhabdomeres of backswimmer contain a pigment with an absorption maximum at 560 nm (Schwind *et al.*, 1984). This is associated with adaptation of the spectral sensitivity of the peripheral visual cells to the illumination conditions in the bodies of water inhabited by *N. glauca*. Backswimmer prefers turbid, still water with a dense growth of aquatic plants (Giller & McNeill, 1981). Under incident daylight the intensity maximum of the scattered background light in bodies of water containing phytoplankton in high concentrations is at 560 nm

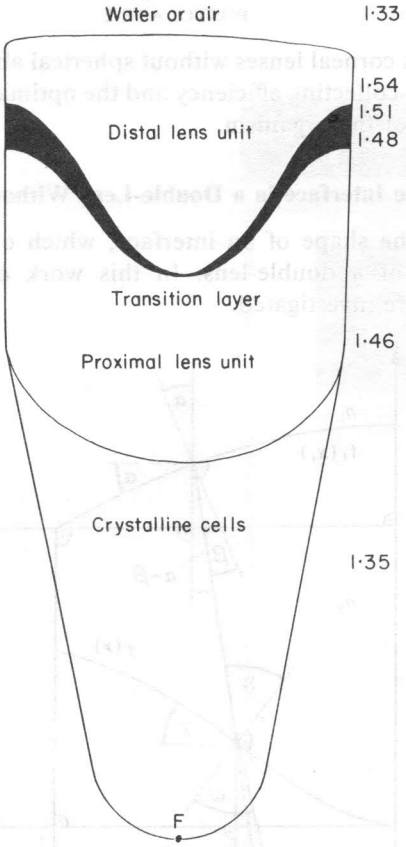

FIG. 1. Refractive indices of the dioptric apparatus of backswimmer. Between two homogeneous lens units there is a thin bell-shaped transition layer within which refractive index changes continuously.

(Lythgoe, 1972). The peripheral rhabdomeres serve as a scotopic system, they are used for perception of dim light in turbid water (Schwind *et al.*, 1984). From these the following can be postulated.

POSTULATE 1

The chromatic aberration of the backswimmer's corneal lens is very small because of the quasi-monochromatic (~560 nm) property of the light in bodies of water perceived by *N. glauca*. This small chromatic aberration can be neglected, because the absorption maximum of the visual pigments of peripheral rhabdomeres of the bug coincides with the emission maximum of the scattered background light in its water environment.

The diameter of the backswimmer's corneal lenses is so small (40 μm) that smaller lenses would not be suitable, because the amount of the light received by an individual cornea is quite small in dim light (Schwind, 1985).

POSTULATE 2

The backswimmer's corneal lenses without spherical aberration serve the purpose of increasing the light-collecting efficiency and the optimal high contrast which have relevance to survival of the organism.

3. The Shape of the Interface in a Double-Lens Without Spherical Aberration

First I determine the shape of an interface, which eliminates the longitudinal spherical aberration of a double-lens. In this work only lenses with radially-symmetric structure are investigated.

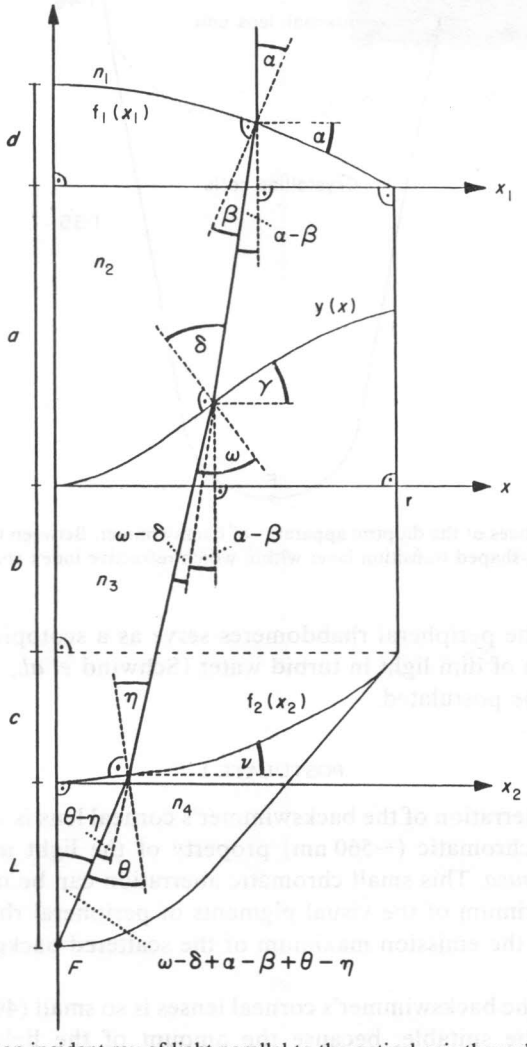

FIG. 2. The path of an incident ray of light parallel to the optical axis through the dioptric apparatus of backswimmer. Only half of the cross-section is represented.

In Fig. 2 the path of a ray of light through the dioptric apparatus of backswimmer can be seen. The incident ray of light is parallel to the optical axis of the lens, because longitudinal spherical aberration is investigated. The refractive indexes of the medium in contact with the entrance surface, the distal and proximal lens units, and the crystalline cells are n_1, n_2, n_3 and n_4, respectively. First I consider the thin transition layer as exact geometrical interface.

The entrance and exit surfaces of the lens and the transition interface can be described (in main section) by the functions $f_1(x_1)$, $f_2(x_2)$ and $y(x)$, respectively, in the system of co-ordinates of Fig. 2. The definition of geometric parameters *a*, *b*, *c*, *d*, *r* and *L* can be read in Fig. 2. The numerical value of these parameters and the refractive indices can be found in Table 1 for the backswimmer's dioptric apparatus.

TABLE 1

Numerical value of the refractive indices and the geometric parameters of the dioptric apparatus of backswimmer (*Schwind*, 1980)

n_1(water) = 1·33 or n_1(air) = 1,	$n_2 = 1{\cdot}54$,	$n_3 = 1{\cdot}46$,	$n_4 = 1{\cdot}35$		
$a = 23\ \mu m$,	$b = 11\ \mu m$,	$c = 12\ \mu m$,	$d = 1\ \mu m$,	$L = 75\ \mu m$,	$r = 20\ \mu m$

The longitudinal spherical aberration is eliminated by the interface. This means that any incident ray parallel to the optical axis crosses the same focal point *F* on the distal tip of the crystalline cells after the refractions. Using the law of refraction and some trigonometrical transformations, the following system of equations can be obtained to calculate the curve $y(x)$ (see Fig. 2).

$$x = x_1 - tg(\alpha - \beta)[f_1(x_1) + a - y(x)], \tag{1}$$

$$x_2 = x - tg(\omega - \delta + \alpha - \beta)[y(x) - a + c - f_2(x_2)], \tag{2}$$

$$L + f_2(x_2) = \frac{x_2}{tg(\Theta - \nu)}, \tag{3}$$

$$tg\delta = \frac{tg(\alpha - \beta) + y'(x)}{1 - tg(\alpha - \beta)y'(x)}, \qquad y'(x) \equiv dy/dx, \tag{4}$$

$$tg\eta = \frac{tg(\omega - \delta + \alpha - \beta) + f_2'(x_2)}{1 - tg(\omega - \delta + \alpha - \beta) \,.\, f_2'(x_2)}, \qquad f_2'(x_2) \equiv \frac{df_2}{dx_2}, \tag{5}$$

$$tg(\alpha - \beta) = \frac{-f_1'(x_1) + \left\{ \dfrac{f_1'(x_1) \,.\, n_1/n_2}{[1 + f_1'^2(x_1)]^{1/2}} \Big/ \left[1 - \dfrac{f_1'^2(x_1) \,.\, (n_1/n_2)^2}{1 + f_1'^2(x_1)} \right]^{1/2} \right\}}{1 + f_1'^2(x_1) \left\{ \dfrac{n_1/n_2}{[1 + f_1'^2(x_1)]^{1/2}} \Big/ \left[1 - \dfrac{f_1'^2(x_1) \,.\, (n_1/n_2)^2}{1 + f_1'^2(x_1)} \right]^{1/2} \right\}}, \tag{6}$$

$$tg(\omega-\delta)=\frac{\left\{\dfrac{tg\delta\,.\,n_2/n_3}{(1+tg^2\delta)^{1/2}}\Big/\left[1-\dfrac{(tg\delta\,.\,n_2/n_3)^2}{1+tg^2\delta}\right]^{1/2}\right\}-tg\delta}{1+\left\{\dfrac{tg^2\delta\,.\,n_2/n_3}{(1+tg^2\delta)^{1/2}}\Big/\left[1-\dfrac{(tg\delta\,.\,n_2/n_3)^2}{1+tg^2\delta}\right]^{1/2}\right\}}, \tag{7}$$

$$tg(\Theta-\nu)=\frac{\left\{\dfrac{tg\eta\,.\,n_3/n_4}{(1+tg^2\eta)^{1/2}}\Big/\left[1-\dfrac{(tg\eta\,.\,n_3/n_4)^2}{1+tg^2\eta}\right]^{1/2}\right\}-f_2'(x_2)}{1+f_2'(x_2)\left\{\dfrac{tg\eta\,.\,n_3/n_4}{(1+tg^2\eta)^{1/2}}\Big/\left[1-\dfrac{(tg\eta\,.\,n_3/n_4)^2}{1+tg^2\eta}\right]^{1/2}\right\}}. \tag{8}$$

The angles used in the above equations can be read in Fig. 2. Introduce the following notation.

$$a_1=f_1'(x_1)[1+f_1'^2(x_1)]^{-1/2}\,.\,n_1/n_2, \qquad a_2=a_1(1-a_1^2)^{-1/2},$$

$$a_3\equiv tg(\alpha-\beta)=\frac{a_2-f_1'(x_1)}{1+a_2f_1'(x_1)}, \qquad f_1'(x_1)\equiv\frac{df_1}{dx_1}. \tag{9}$$

$$b_1=\frac{x-x_2}{y-a+c-f_2(x_2)}, \qquad b_2=\frac{b_1-a_3}{1+b_1a_3}, \qquad b_3=\frac{b_1+f_2'(x_2)}{1-b_1f_2'(x_2)},$$

$$b_4=b_3(1+b_3^2)^{-1/2}\,.\,n_3/n_4, \qquad b_5=(1-b_4^2)^{1/2},$$

$$b_6=b_4/b_5-f_2'(x_2), \qquad b_7=1+f_2'(x_2)b_4/b_5. \tag{10}$$

From eqns (1), (3) and (7) we obtain.

$$F(x_1)\equiv x_1-x-a_3[f_1(x_1)+a-y]=0 \tag{11}$$

$$G(x_2)\equiv L+f_2(x_2)+x_2b_7/b_6=0 \tag{12}$$

$$H(t)\equiv t^4\left[1-\frac{n_2^2}{n_3^2}(1+b_1^2)\right]+2t^3b_1+t^2\left(1-\frac{n_2^2}{n_3^2}\right)(1+b_1^2)$$
$$+2tb_1+b_1^2=0, \qquad t\equiv tg\delta. \tag{13}$$

From eqn (4) we obtain

$$y'(x)=\frac{t-a_3}{1+ta_3}. \tag{14}$$

The system of eqns (1–8) can then be solved in the following way. First we solve eqn (11) for x_1 numerically, using the tangent recursive formula of Newton:

$$x_1^{(i+1)}=x_1^{(i)}-\frac{F[x_1^{(i)}]}{F'[x_1^{(i)}]}, \qquad F'(x_1)\equiv\frac{dF}{dx_1} \tag{15}$$

for the approximate roots $x_1^{(i)}$. Then we solve eqns (12) and (13) numerically for x_2 and t, respectively, using the recursions

$$x_2^{(i+1)}=x_2^{(i)}-\frac{G[x_2^{(i)}]}{G'[x_2^{(i)}]}, \qquad G'(x_2)\equiv\frac{dG}{dx_2}, \tag{16}$$

$$t^{(i+1)}=t^{(i)}-\frac{H[t^{(i)}]}{H'[t^{(i)}]}, \qquad H'(t)\equiv\frac{dH}{dt}. \tag{17}$$

Then substituting the root x_1 into the expression of a_3, then substituting the root t and a_3 into eqn (14) we obtain $y'(x)$. Using the boundary condition

$$y(x=0)=0, \tag{18}$$

we can determine the curve $y(x)$, because it is

$$y(x+\Delta x)=y(x)+y'(x)\,.\,\Delta x, \qquad \Delta x=r/m, \tag{19}$$

where r is the radius of the lens, and m is a large number. The larger the number m is, the better the numerical solution for $y(x)$ is.

4. Theoretical Transition Layers of Differently Shaped Amphibious lenses

I apply the above geometric optical method for differently shaped lenses, the entrance and/or exit surfaces of which can be described in the following way

$$\text{plane:} \quad f_1(x_1)=f_2(x_2)=0, \tag{20}$$

$$\text{paraboloid:} \quad f_1(x_1)=d-d(x_1/r)^2, \qquad f_2(x_2)=c(x_2/r)^2, \tag{21}$$

$$\text{ellipsoid:} \quad f_1(x_1)=d[1-(x_1/r)^2]^{1/2}, \qquad f_2(x_2)=c-c[1-(x_2/r)^2]^{1/2}, \tag{22}$$

and the medium in contact with the entrance surface is water or air (amphibious lenses).

I substituted eqns (20), (21) or (22) into the system of eqns (1-8) and solved it using the method presented above. The results can be seen in Figs 3-11. I varied

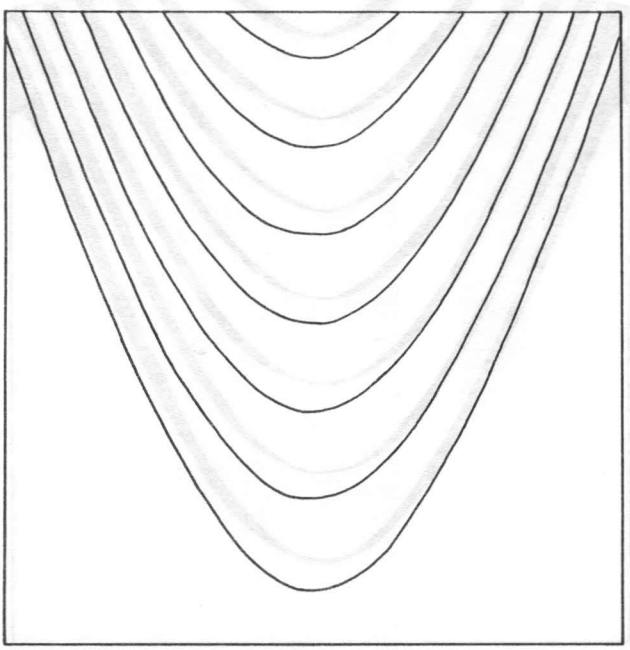

FIG. 3. Theoretical transition layers in the plane-parallel cornea.

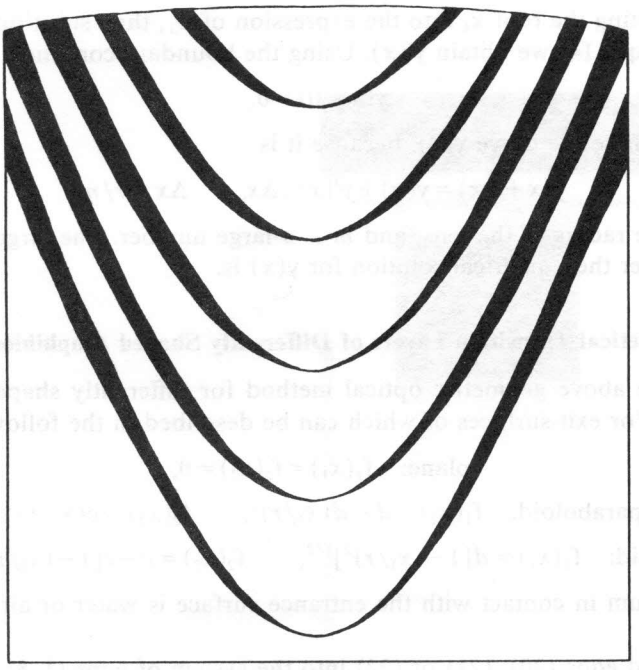

FIG. 4. Theoretical transition layers in the paraboloid-plane cornea.

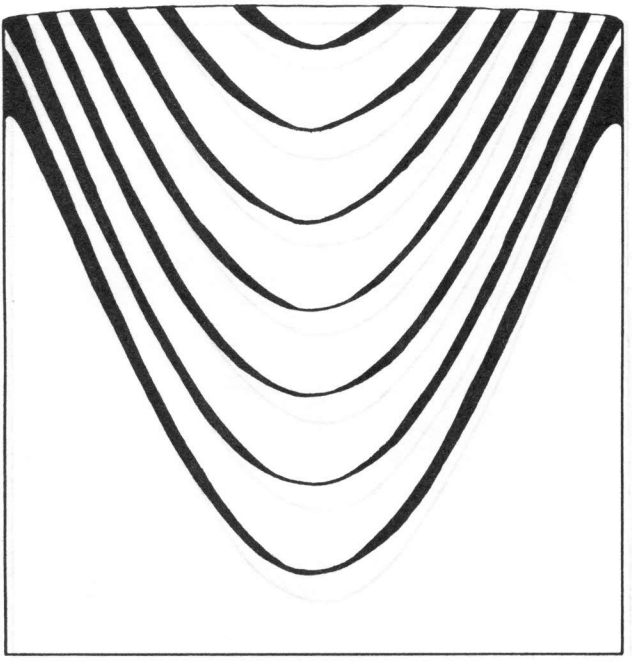

FIG. 5. Theoretical transition layers in the ellipsoid-plane cornea.

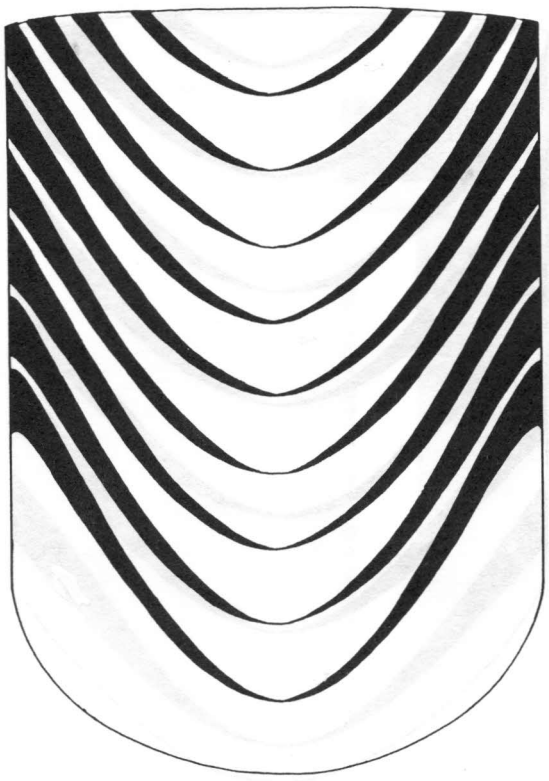

FIG. 6. Theoretical transition layers in the paraboloid-ellipsoid cornea.

the geometrical parameter a, and obtained a family of curves for $y(x)$. The shape of the theoretical interface depends on the refractive index n_1, if the entrance surface of the lens is not a plane and is not perpendicular to the axis of the ommatidium. The upper boundaries of the transition layers in Figs 4–7, 10 and 11 are the theoretical interfacial curves for $n_1(\text{water}) = 1{\cdot}33$, and the lower ones are those for $n_1(\text{air}) = 1$.

The shape of the interfaces for air differs from those for water. If only an interface existed in the cornea of backswimmer and its shape agreed with that of the theoretical interface determined for $n_1(\text{water}) = 1{\cdot}33$, for example, then the corneal lens would not have longitudinal spherical aberration in water, but it would have large spherical aberration in air. It is more advantageous when a layer of finite thickness exists in the cornea, its boundaries are the interfaces determined for water and air, and the refractive index varies continuously in it. In this case the corneal lens has a little spherical aberration in air and water, but it is much smaller than it would be if only an interface existed.

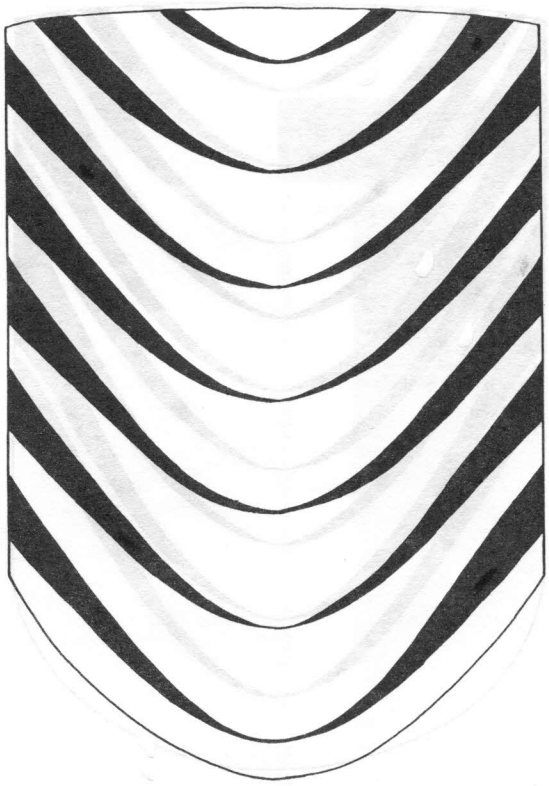

FIG. 7. theoretical transition layers in the paraboloid-paraboloid cornea.

POSTULATE 3

The optimal transition layer in the cornea of amphibious *N. glauca* is the zone between the theoretical interfaces determined for water and air, and the refractive index varies continuously in it.

5. The Optimal Shape of the Backswimmer's Cornea

In Figs 3–11 the radius of the lenses is $r = 20$ μm, like that of backswimmer. Only that transition layer which does not reach the entrance surface can eliminate the spherical aberration for the whole of the lens.

POSTULATE 4

The transition layer cannot reach the entrance surface of the backswimmer's cornea, or else the diameter of the spherically corrected lens would be smaller. If the thickness of the transition layer is large, the corneal lens has large spherical aberration.

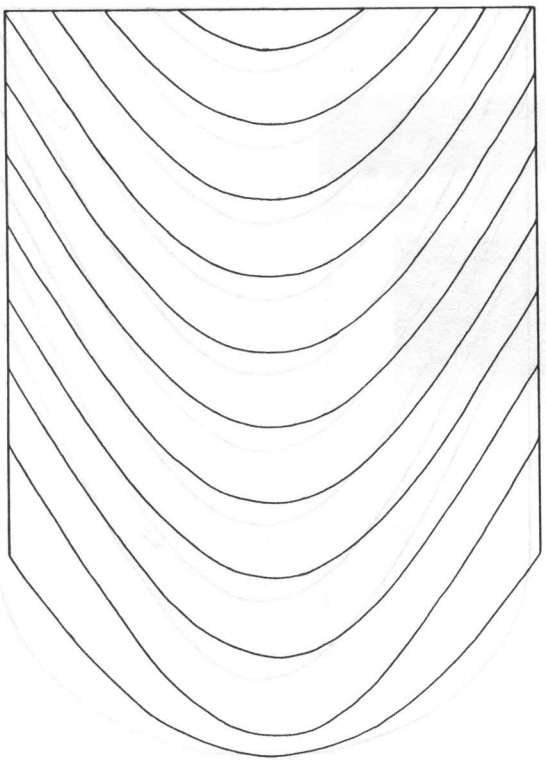

FIG. 8. Theoretical transition layers in the plane-paraboloid cornea.

POSTULATE 5

A thinner transition layer in the backswimmer's cornea is more advantageous than a thicker one, considering the spherical aberration.

A transition interface has infinite gradient of refractive index, therefore the amount of reflected light from it is large. This decreases the light-collecting efficiency of the lens.

POSTULATE 6

Transition interface in the corneal lens of backswimmer is rejected because of the large amount of reflected light.

The amount of reflected light from the transition layer is large when the angle between the incident rays and the normal vector of the layer is large.

POSTULATE 7

It is disadvantageous when the rise of the transition layer in the backswimmer's cornea is large, because the amount of the reflected light is large.

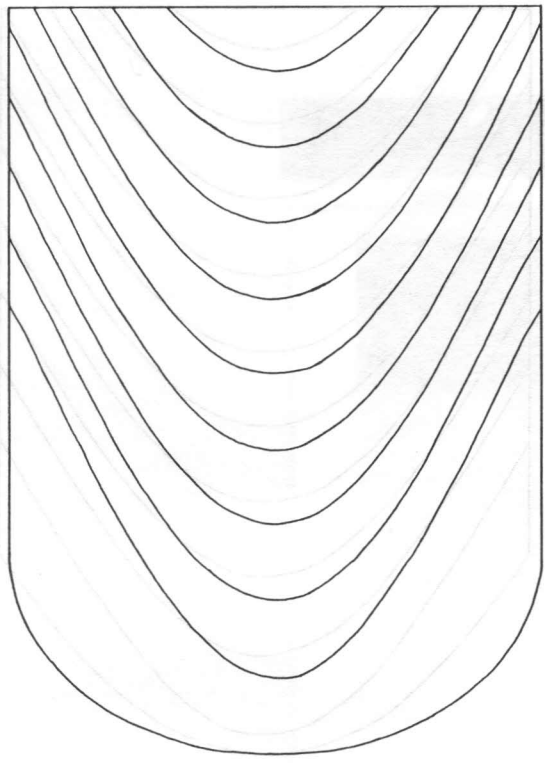

FIG. 9. Theoretical transition layers in the plane-ellipsoid cornea.

On the basis of the former the optimal shape of the backswimmer's corneal lens can be determined. I apply the above postulates for Figs 3–11, and reject the disadvantageously-shaped lenses. I seek a lens of which the transition layer, defined by postulate 3, has optimal properties considering postulate 2.

Due to postulate 1, elimination of chromatic aberration is not needed: therefore two lens units with a thin transition layer are sufficient for the backswimmer. In the plane-parallel, paraboloid-plane and ellipsoid-plane lenses (Figs 3, 4 and 5, respectively), all the transition layers reach the entrance surface, because the boundary surfaces are very flat: therefore abrupt transition layers are needed for focusing. Considering postulates 4 and 7 we can reject those corneal lenses of which the exit surface is plane. In the paraboloid-ellipsoid and paraboloid-paraboloid lenses (Figs 6 and 7, respectively) the transition layers are thicker than in the case of the other lenses investigated (see Figs 8–11). On the basis of postulate 5 these disadvantageous corneal lenses are rejected.

In the plane-paraboloid and plane-ellipsoid lenses (Figs 8 and 9, respectively), the theoretical transition layers are interfaces, the shape of which does not depend on the refractive index of the medium in contact with the entrance surface. These interfaces are rejected considering postulate 6. They are very abrupt near the margin

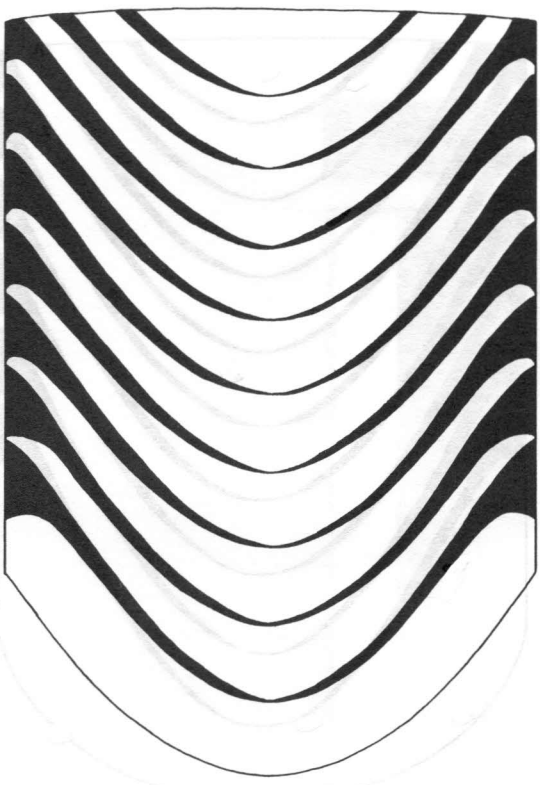

FIG. 10. Theoretical transition layers in the ellipsoid-paraboloid cornea.

of the cornea, therefore they are disadvantageous also considering postulate 7. So corneal lenses with plane entrance surface are rejected. It can be seen in Figs 10 and 11 that the bell-shaped transition layers of the ellipsoid-paraboloid lens are thicker than those of the ellipsoid-ellipsoid one. Considering postulate 6 the former lens is rejected.

In sum the ellipsoid-ellipsoid lens and its thin bell-shaped transition layers (Fig. 11) are the optimal for the water bug *N. glauca* with respect to the spherical aberration and the amount of reflected light. It can be seen in Fig. 11 that the shape of the optimal ellipsoid-ellipsoid corneal lens and its transition layers are very similar to the real ones of backswimmer (see Fig. 1).

6. The Optimal Position of the Transition Layer in the Backswimmer's Cornea

I determine the optimal value of the geometrical parameter a in the cornea of *N. glauca*, considering the bell-shaped theoretical transition layers in the ellipsoid-ellipsoid corneal lens. Layers 1, 2, 3 and 4 in Fig. 11 are rejected on the basis of postulate 4. In Fig. 12 the connection of two ellipsoid-ellipsoid corneal lenses with the marginal connection of the non-rejected theoretical transition layers can be seen.

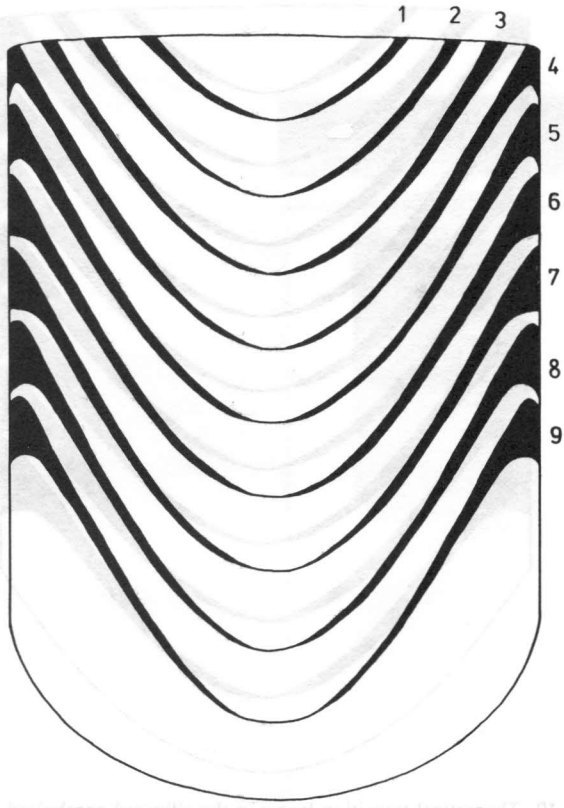

FIG. 11. Theoretical transition layers in the ellipsoid-ellipsoid cornea.

The maxima of the fourth degree boundary surfaces of these layers are just on the margin for layers 6 and 7, and near the margin for layers 5, 8 and 9: therefore there is a dimple at the marginal connection of the latter layers. The size of these dimples is comparable with the wavelength of 560 nm (see Fig. 12), so the diffraction of light becomes large on these dimples. There is no dimple at the marginal connection of layers 6 and 7, thus there is no diffraction on these connections. Also diffraction of light depreciates the light-collecting efficiency and the high contrast imaging of the lens, therefore it is disadvantageous considering postulate 2.

POSTULATE 8

A marginal connection of the transition layers in the backswimmer's cornea with dimples, the size of which is comparable to the sensitivity maximum of peripheral visual receptors of the bug (560 nm), is disadvantageous because of the diffraction.

Considering postulate 8, layers 5, 8 and 9 in the ellipsoid-ellipsoid cornea are rejected. The optimal position of the transition layer in the backswimmer's cornea

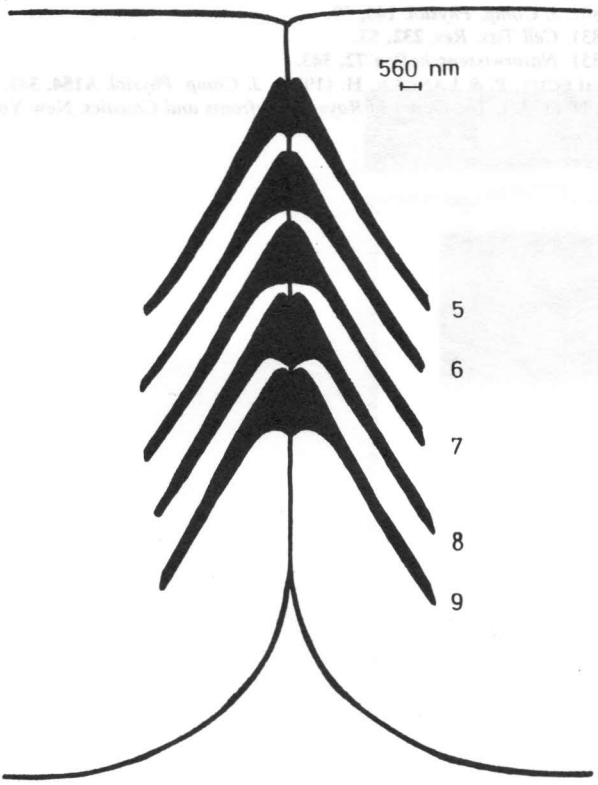

FIG. 12. A marginal connection of two ellipsoid-ellipsoid corneal lenses with the marginal connections of the theoretical transition layers.

can be found between the position of layers 6 and 7 (Fig. 12). The geometrical parameter a of a transition layer between these layers is approximately equal to that in *N. glauca* ($a = 23$ μm).

Thanks are due to Professor Rudolf Schwind (Institut für Zoologie der Universität Regensburg) and Professor Pál Greguss (Applied Biophysical Laboratory, Technical University, Budapest) for their help, advice and support.

REFERENCES

BORN, M. & WOLF, E. (1964). *Principles of Optics.* Oxford: Pergamon Press.
CHANG, R. S. & STRAVROUDIS, O. N. (1980). *J. Opt. Soc. Am.* **70,** 976.
CLARKSON, E. N. K. (1973). *Paleontology* **16,** 425.
GILLER, P. & MCNEILL, S. (1981). *J. Anim. Ecol.* **50,** 798.
LEVI-SETTI, R. (1975). In: *Trilobites* (*A photographic atlas*). p. 213 Chicago; London: The University Chicago Press.
LUNEBURG, R. K. (1964). *Mathematical Theory of Optics.* Berkeley: University of California Press.
LYTHGOE, J. N. (1972). In: *Photochemistry of vision. Handbook of sensory physiology. Vol. VII*/1. (Dartnall, H. J. A., ed.) pp. 566–603. Berlin, Heidelberg, New York: Springer-Verlag.

SCHWIND, R. (1980). *J. Comp. Physiol.* **140,** 59.
SCHWIND, R. (1983). *Cell Tiss. Res.* **232,** 53.
SCHWIND, R. (1985). *Naturwissenschaften* **72,** 343.
SCHWIND, R., SCHLECHT, P. & LANGER, H. (1984). *J. Comp. Physiol.* **A154,** 341.
STRAVROUDIS, O. N. (1972). *The Optics of Rays, Wavefronts and Caustics.* New York: Academic Press.